Journal of Magnetic Resonance **139,** 377–381 (1999)
Article ID jmre.1999.1794, available online at http://www.idealibrary.com on IDEAL®

^{13}C Selective Polarization and Spin Diffusion in a Lipid Bilayer-Bound Polypeptide by Solid-State NMR

Fang Tian,*,[1] Riqiang Fu,* and Timothy A. Cross*,†,[2]

*Center for Interdisciplinary Magnetic Resonance, National High Magnetic Field Laboratory, and †Department of Chemistry, Institute of Molecular Biophysics, Florida State University, Tallahassee, Florida 32310

Received January 26, 1999; revised April 13, 1999

While ^{15}N solid-state NMR has proven to be very advantageous for the development of structural biological methods, ^{13}C spectroscopy has increased sensitivity and spectral dispersion. However, large natural abundance signals and homonuclear dipolar interactions pose significant problems. Here we have used a pair of ^{13}C-labeled sites in a lipid-solubilized polypeptide to show the selective polarization can be used in combination with spin diffusion to achieve simplified spectra. Both unoriented and oriented samples have been used, with the latter providing a well-resolved homonuclear dipolar splitting. © 1999 Academic Press

Key Words: **solid-state NMR; selective polarization; spin diffusion; polypeptide; orientational constraints.**

Resolution in solid-state ^{13}C NMR spectra of specific site labels in a background of natural abundance is very challenging for all but the smallest biological molecules. Particularly, the observation of a labeled polypeptide in unoriented and oriented lipid bilayer preparations poses a very severe problem. Yet in comparison with ^{15}N, ^{13}C is a relatively sensitive nucleus and it possesses favorable relaxation properties for homonuclear spin diffusion. While spin diffusion is the scourge of many NMR experiments here it can be used to observe homonuclear dipolar interactions and to potentially make resonance assignments. In the present work, a combination of selective polarization and spin exchange techniques has been applied to observe $^{13}C_\alpha$–$^{13}C_1$ homonuclear dipolar splitting from a membrane-bound polypeptide while suppressing natural abundance signals from the lipid carbonyl carbon resonances.

A standard pulse sequence for two-dimensional (2D) spin diffusion experiments with cross-polarization preparation is shown in Fig. 1. However, a contact time of a few tens of microseconds instead of a few milliseconds has been used to selectively polarize the protonated versus nonprotonated carbons. Fortunately, such a relatively short contact time may lead to better sensitivity for the protonated carbons because of the strong couplings between the carbons and the attached protons, especially for systems having a short proton $T_{1\rho}^{H}$ relaxation. This is based on transient dipolar oscillation phenomena as described before (*1, 2*). For the selectively $^{13}C_\alpha$–$^{13}C_1$-labeled polypeptide, $^{13}C_\alpha$ but not $^{13}C_1$ is polarized. Following cross-polarization the $^{13}C_\alpha$ magnetization evolves during the evolution period t_1. A 90° pulse is applied to restore the $^{13}C_\alpha$ magnetization along the z axis before the mixing time τ_m, during which the magnetization is transferred from $^{13}C_\alpha$ to $^{13}C_1$ through proton-driven carbon–carbon spin diffusion in the absence of proton decoupling. The spin–lattice relaxation effect during the mixing time is alleviated by storing the magnetization alternatively along the $+Z$ and $-Z$ directions (*3*). Another 90° pulse brings the longitudinal ^{13}C magnetization back into the transverse plane for signal observation during the detection period t_2. For one-dimensional experiments, the evolution period t_1 is set to zero.

The selectivity of polarizing protonated carbon versus nonprotonated carbon through transient oscillation depends on the magnitude difference of the dipolar interaction between the protonated carbon and the bonded protons and that between the nonprotonated carbon and nearby protons. For the protonated carbon (e.g., $^{13}C_\alpha$) where strong heteronuclear proton–carbon dipolar interactions are present, the cross-polarized $^{13}C_\alpha$ magnetization experiences a dipolar oscillation during the cross-polarization in these hydrated bilayer preparations (*2*). The buildup of the $^{13}C_\alpha$ magnetization can be characterized by $T_{1\rho}^{H}$, proton–proton spin diffusion rate R and the static magnitude of the dipolar interaction b (*1*):

$$M(t) = M_0 e^{-t/T_{1\rho}^{H}}\left(1 - 0.5e^{-Rt} - 0.5e^{-1.5Rt}\cos\frac{bt}{2}\right). \quad [1]$$

On the other hand, because the protons involved in the cross-polarization are further away from the carbonyl carbon, the buildup of the cross-polarized $^{13}C_1$ magnetization is rather slow and no dipolar oscillations are expected during cross-polarization. The polarized $^{13}C_1$ magnetization can be described using the following expression (*4*) with the assumption of a very long $^{13}C_1$ longitudinal relaxation time in the doubly rotating frame:

[1] Present address: Complex Carbohydrate Research Center, University of Georgia, Athens, GA 30602.

[2] To whom correspondence should be addressed.

1090-7807/99 $30.00

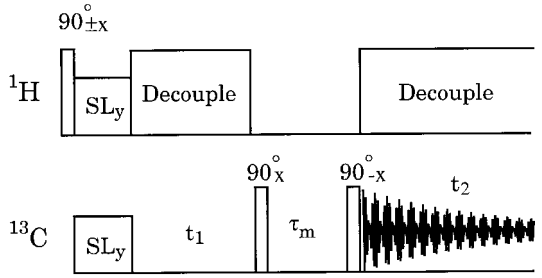

FIG. 1. Pulse sequence for proton-mediated ^{13}C spin diffusion while suppressing the natural abundance ^{13}C signal from lipid carbonyl carbons. The spin lock (SL) is restricted to tens of microseconds so as to selectively polarize the protonated ^{13}C.

$$M(t) = M_0 e^{-t/T_{1\rho}^{H}}(1 - e^{-\lambda t/T_{C_1H}}). \quad [2]$$

Here, $\lambda = 1 - T_{C_1H}/T_{1\rho}^{H}$ and T_{C_1H} is the cross-relaxation time between the $^{13}C_1$ and bulk protons involved in the cross-polarization process. In the system studied here, the $^{13}C_\alpha$–H heteronuclear dipolar coupling for glycine residues is 22.5 kHz. We can reasonably assume that $T_{1\rho}^{H} = 5.4$ ms and $R^{-1} = 280$ μs as obtained before (*2*), and T_{C_1H} is considered to be ~450 μs (*5*). Thus, a factor of 10 in selectivity for the protonated site can be achieved by using a 15-μs contact time. A longer contact time will deteriorate the selectivity. For instance, a 25-μs contact time generates a factor of 7.5 in selectivity. Although the selectivity is not great, it is sufficient to suppress the lipid carbonyl carbon resonances. This may be partially due to the high peptide:lipid molar ratio (1:8) used in the sample preparations. For systems where more dilute peptide:lipid ratios are needed, the signals from the lipid carbonyl carbons can be further suppressed by incorporating other selective excitation techniques. For example, a shaped pulse can be easily applied because the carbonyl carbon resonances are more than 100 ppm away from the $^{13}C_\alpha$ resonance (*6*).

Chemical shift spectra of a labeled $^{13}C_{1,\alpha}$–Gly_2 gramicidin A in hydrated unoriented dimyristoylphosphatidylcholine (DMPC) bilayers recorded at 36°C are shown in Fig. 2. A spectrum using a standard cross-polarization experiment is presented in Fig. 2A. The $^{13}C_\alpha$ signal is between 40 and 60 ppm, buried in the natural abundance ^{13}C signals from the lipids. The signals around 170 ppm result from the superposition of the chemical shift powder pattern from the lipid backbone and isotopically labeled carbonyl carbons in the peptide. Both chemical shift tensors are extensively averaged by fast global motions of the polypeptide and lipid about the bilayer normal (*7*) which is parallel to the applied magnetic field. For the Gly_2 site in gramicidin the static chemical shift tensor has the $\sigma_{11} = 242$ ppm element in the peptide plane with $\sigma_{22} = 173$ ppm also in the plane and making an angle of 20° with respect to the carbonyl bond, while $\sigma_{33} = 91$ ppm is perpendicular to the peptide plane (*8*). With a peptide:lipid molar ratio of 1:8, approximately 70% of the carbonyl signal is from the single-site label while the natural abundant signal is contributed in equal parts from the polypeptide and lipid. Furthermore, this carbonyl region is complicated by the $^{13}C_\alpha$–$^{13}C_1$ homonuclear dipolar interaction. However, from the known structure of the polypeptide the C_α–C_1 bond of the glycine residue makes an angle of 56° with respect to the channel axis, corresponding to a predicted dipolar splitting of 236 Hz (2.4 ppm at 9.4 T) for the parallel component based on a $^{13}C_\alpha$–$^{13}C_1$ dipolar coupling

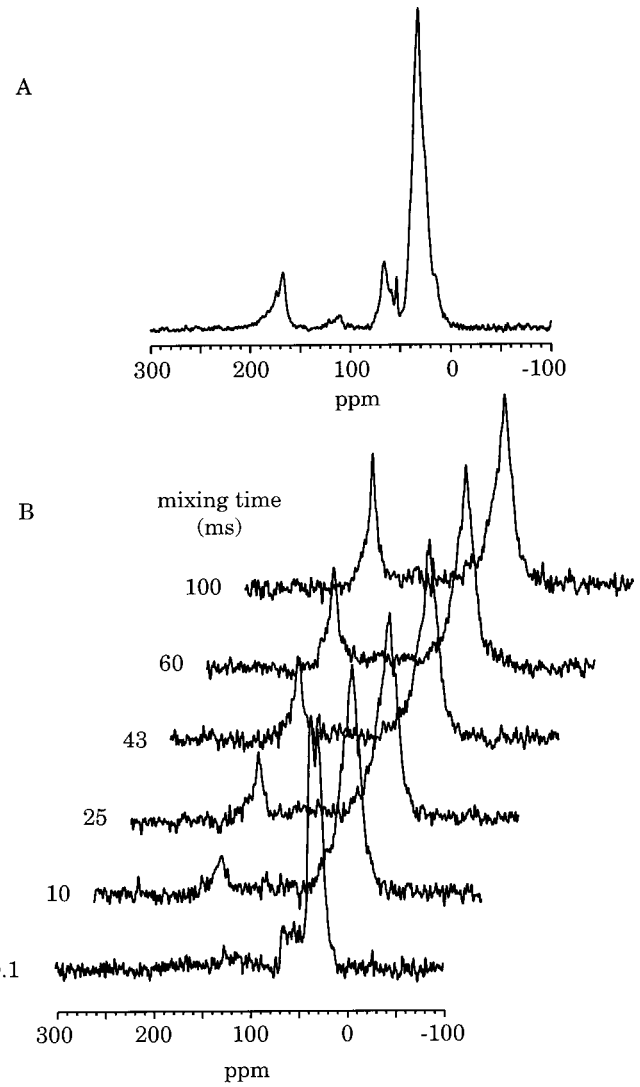

FIG. 2. ^{13}C chemical shift spectra of 40 mg $^{13}C_{1,\alpha}$-Gly_2 gramicidin A in hydrated unoriented DMPC bilayers (peptide:lipid molar ratio = 1:8) recorded on a 400-MHz homebuilt spectrometer at 36°C. The ^{13}C chemical shifts were referenced at 38.0 ppm to adamantine. (A) Spectrum recorded by a cross-polarization pulse sequence with 1-ms contact time, 4-s recycle delay, and 8512 scans. (B) Stacked plot of series spectra with various mixing times recorded by the pulse sequence shown in Fig. 1 ($t_1 = 0$). Each of them was acquired with 25-μs contact time, 4-s recycle delay, and 6000 scans. Gramicidin A is a linear polypeptide of 15-amino-acid residues, which as a dimer forms selective monovalent cation conducting channels across lipid membranes (*21, 22*). The high-resolution three-dimensional structure of gramicidin A has been solved from orientational constraints by solid-state NMR (*18, 23*).

constant of 2.12 kHz using a C–C bond length of 1.53 Å. Such a weak coupling results in an unresolved dipolar powder pattern superimposed on a broadening of the chemical shift powder pattern. No evidence exists in this spectrum for a splitting of 1.9 kHz previously reported for this site (*9*). This latter study faced considerable challenges using oriented samples and suffered from linewidths of 2 kHz. The data may have been overinterpreted.

Figure 2B is a stacked plot of spectral series with different mixing times for spin exchange recorded using the pulse sequence shown in Fig. 1 ($t_1 = 0$). A 25-μs contact time was used for selective polarization of the protonated carbons. The carbonyl signal was not observed when the mixing time was very short (e.g., 100 μs), indicating that the carbonyl carbons were barely cross-polarized. However, a carbonyl signal does build up when the mixing time is increased as shown in Fig. 2B. The exchange process was nearly completed at a mixing time of ~100 ms. Since the intrinsic longitudinal relaxation rates for $^{13}C_\alpha$ and $^{13}C_1$ in this sample were not measured, the experimental data were not simulated (*10, 11*). Spin diffusion from the methylene carbons toward the carbonyl carbons along the lipid chain is not visible with the mixing times used in these experiments (spectra not shown) because the natural abundance occurrence of any specific $^{13}C_\alpha$–$^{13}C_1$ pairs is 10^{-4}. Furthermore, the polypeptide backbone is effectively separated from the lipid chain by its side chains so that polarization transfer from the labeled $^{13}C_\alpha$–Gly_2 gA to the carbonyl carbons in the lipid bilayers cannot occur during the given mixing times. Consequently, the carbonyl intensity in Fig. 2B is undoubtedly that from the labeled site, despite the relatively weak $^{13}C_\alpha$–$^{13}C_1$ dipolar interaction for this site. The spin diffusion rate between two spins depends on their distance, the orientation of the internuclear vector with respect to the magnetic field direction, and the overlap of the two proton-coupled resonances (*12*). The very efficient carbon–carbon spin diffusion could potentially be applied to assign the resonances in uniformly labeled samples. In fact, ^{13}C–^{13}C spin diffusion has been incorporated to assign a fully $^{13}C/^{15}N$ labeled polypeptide in a recent MAS study recently (*13*).

In the 2D spin exchange experiments, the intensities of the diagonal and cross-peaks can be written as (*14*)

$$I_{AA}(\tau_m) = \frac{1}{2}\left[\left(1 - \frac{\delta}{D}\right) + \left(1 + \frac{\delta}{D}\right)\exp(-2D\tau_m)\right] \times \exp[-(\sigma - D)\tau_m]M_0(A), \quad [3]$$

$$I_{BB}(\tau_m) = \frac{1}{2}\left[\left(1 + \frac{\delta}{D}\right) + \left(1 - \frac{\delta}{D}\right)\exp(-2D\tau_m)\right] \times \exp[-(\sigma - D)\tau_m]M_0(B), \quad [4]$$

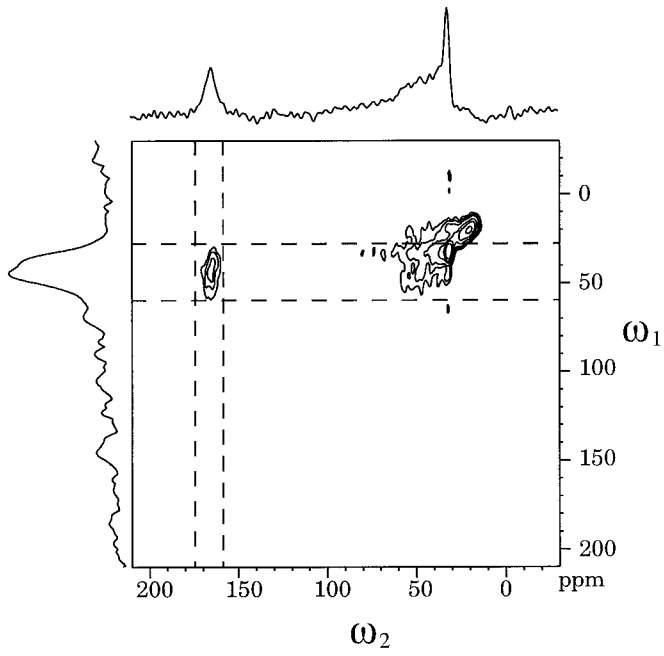

FIG. 3. ^{13}C 2D spectrum of labeled $^{13}C_{1,\alpha}$–Gly_2 gramicidin A in hydrated unoriented DMPC bilayers recorded at 36°C by the pulse sequence shown in Fig. 1. The cross-peak region is highlighted by vertical and horizontal dashed lines. The projections of the area between the two dashed lines in the ω_1 and ω_2 dimensions are shown at the left and on the top of the contour plot. The spectrum was recorded on a Bruker DMX300 WB spectrometer with a 15-μs contact time and 60-ms mixing time. Five hundred twelve points were taken in the t_2 domain and 320 scans were coadded for each of 64 t_1 experiments with a 22-μs dwell time in both dimensions.

$$I_{AB}(\tau_m) = \frac{1}{2}[1 - \exp(-2D\tau_m)] \times \exp[-(\sigma - D)\tau_m]M_0(B)\frac{k}{D}, \quad [5]$$

$$I_{BA}(\tau_m) = \frac{1}{2}[1 - \exp(-2D\tau_m)] \times \exp[-(\sigma - D)\tau_m]M_0(A)\frac{k}{D}, \quad [6]$$

where $\sigma = \frac{1}{2}(2k + R_1^A + R_1^B)$, $\delta = \frac{1}{2}(R_1^A - R_1^B)$, $D = [\delta^2 + k^2]^{1/2}$, M_0 is the initial transverse magnetization after cross-polarization, τ_m is the mixing time, and R_1 is the spin–lattice relaxation rate while k is the spin diffusion rate between spins A and B. Here A and B stand for $^{13}C_\alpha$ and $^{13}C_1$, respectively. A 2D spectrum with selective cross-polarization is shown in Fig. 3, further indicating that the observed carbonyl signal in Fig. 2B comes from spin exchange. Since the carbonyl carbons were not polarized, i.e., $M_0(B) = 0$, no diagonal peak for the carbonyl carbon resonance (i.e., $I_{BB} = 0$) was observed, resulting in the lack of the lower right cross-peak in the 2D contour ($I_{BA} = 0$). In fact, the absence of the strong, uninfor-

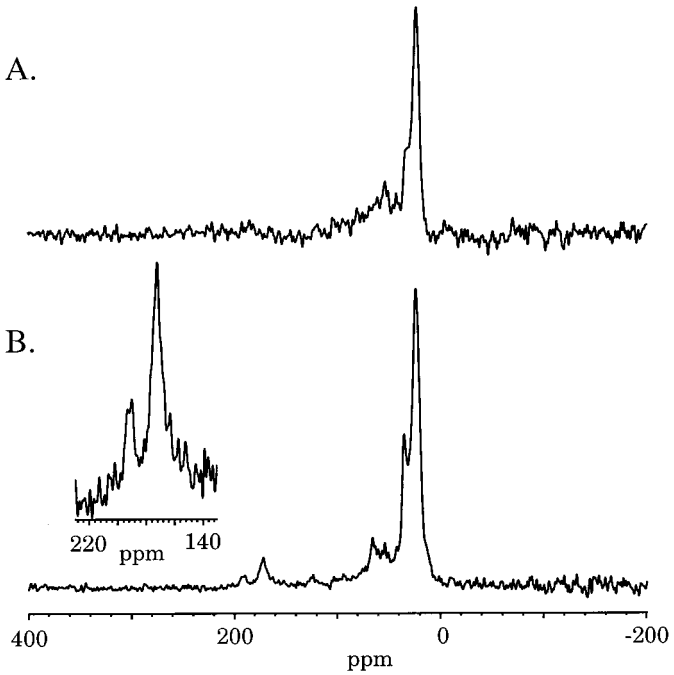

FIG. 4. ^{13}C chemical shift spin exchange spectra on 10 mg $^{13}C_{1,\alpha}$-Ala_3 gramicidin A in oriented DMPC bilayers (peptide:lipid molar ratio = 1:32) recorded on a 400-MHz homebuilt spectrometer at 36°C using the pulse sequence shown in Fig. 1 ($t_1 = 0$). The spin lock time was 25 μs and the recycle time 4 s: (A) 100-μs mixing time and 16,912 scans; (B) 80-ms mixing time and 32,422 scans.

mative diagonal peak is favorable. Since the exchange cross-peak usually is weak, any phase or baseline imperfections caused by the strong diagonal signals can seriously interfere with its observation (*15*). The projections of the observed cross-peak in the ω_1 and ω_2 domains represent signals from labeled $^{13}C_\alpha$ and $^{13}C_1$.

Chemical shift spectra of a labeled $^{13}C_{1,\alpha}$-Ala_3 gramicidin A in oriented DMPC bilayers recorded with the pulse sequence in Fig. 1 ($t_1 = 0$) are shown in Fig. 4. A 25-μs contact time was used. Again, when the mixing time was short (e.g., 100 μs), no signal was observed between 170 and 200 ppm in the carbonyl region (cf. Fig. 4A). However, when the mixing time was increased to 80 ms, a $^{13}C_\alpha$–$^{13}C_1$ homonuclear dipolar splitting of 2.0 $\pm$ 0.3 kHz is observed owing to carbon–carbon spin diffusion. The chemical shift for the single-site $^{13}C_1$-Ala_3-labeled gramicidin is 182 ppm (*16*), and here for the doubly labeled sample two resonances are observed at 172 and 192 ppm. The asymmetry in the intensity of these two resonances is most likely due to a cross-correlation relaxation effect between the ^{13}C–^{13}C dipolar interaction and the chemical shift anisotropy (*17*). Such asymmetry has frequently been observed in similar samples with ^{15}N–^2H and ^{15}N–^{13}C dipolar interactions (*18*, *19*).

The observed homonuclear dipolar splitting can be described as (*3*)

$$\Delta\nu_{\text{obs}} = \tfrac{3}{2}\, b(3\cos^2\theta - 1), \qquad [7]$$

where b is the static magnitude of the dipolar interaction and θ is the orientation of the internuclear vector with respect to the magnetic field direction. Therefore, the $^{13}C_\alpha$–$^{13}C_1$ homonuclear dipolar interaction can provide an important orientational constraint for the peptide plane. The observed splitting of 2.0 kHz for Ala_3 $^{13}C_\alpha$–$^{13}C_1$ is consistent with a C_α–C_1 bond orientation of either 69.5° $\pm$ 3° or 42.5° $\pm$ 2°. The latter orientation is not consistent with the known structure which predicts an orientation of 76° (*18*). The difference between 69.5° $\pm$ 3° and 76° is attributable to the use of a static magnitude for the dipolar interaction instead of the motionally averaged (due to local librational motions) interaction magnitude. With a high-resolution dynamic description of this site it would be possible to use this constraint in addition to other constraints previously obtained from this peptide plane (e.g., ^{13}C and ^{15}N chemical shifts; ^{15}N–^{13}C and ^{15}N–^1H (^2H) dipolar interactions) to solve for the ω torsion angle. Indeed these axially symmetric dipolar interactions provide an analytical solution for bond orientations, whereas axially asymmetric interactions such as chemical shifts provide only limits to the orientational range.

In summary, the transient oscillation during cross-polarization in hydrated lipid bilayers has been applied to selectively polarize protonated spins permitting the observation of the carbonyl carbon resonances only from the labeled polypeptide. The measured $^{13}C_\alpha$–$^{13}C_1$ homonuclear dipolar interaction without influence from the lipid carbonyl carbons provides an important orientational constraint for structure determination. The efficient spin diffusion between adjacent carbon sites is in contrast to the relatively inefficient spin diffusion between ^{15}N sites in the polypeptide backbone (*20*) and so this more efficient spin diffusion may potentially be useful for resonance assignments in uniformly labeled samples.

ACKNOWLEDGMENTS

The authors are indebted to the staff of the National High Magnetic Field Laboratory and the Florida State University Bioanalytical Synthesis and Services Facility, especially A. Blue, H. Hendricks, and U. Goli, for the expertise and maintenance of the NMR spectrometers, peptide synthesizer and HPLC equipment. This work has been supported by the National Science Foundation (MCB-9603935) and the work has largely been performed at the National High Magnetic Field Laboratory supported by NSF Cooperative Agreement DMR-9527035 and the State of Florida.

REFERENCES

1. L. Müller, A. Kumar, T. Baumann, and R. R. Ernst, Transient oscillations in NMR cross-polarization experiments in solids, *Phys. Rev. Lett.* **32,** 1402–1406 (1974).
2. F. Tian and T. A. Cross, Dipolar oscillations in cross-polarized peptide samples in oriented lipid bilayers, *J. Magn. Reson.* **125,** 220–223 (1997).
3. K. Schmidt-Rohr and H. W. Spiess, "Multidimensional Solid-State NMR and Polymers," Academic Press, San Diego (1994).

4. D. E. Axelson, "Solid State Nuclear Magnetic Resonance of Fossil Fuels," Multiscience, Canada (1985).
5. S. Ding and C. Ye, Corrections to the cross-polarization dynamics in solids: The effect of nonsecular terms of heteronuclear dipolar interaction on cross-relaxation, *Solid State Nucl. Magn. Reson.* **1,** 321–328 (1992).
6. S. K. Straus, T. Bremi, and R. R. Ernst, Resolution enhancement by homonuclear *J* decoupling in solid state MAS NMR, *Chem. Phys. Lett.* **262,** 709–715 (1996).
7. K. C. Lee, W. Hu, and T. A. Cross, ^{2}H NMR determination of the global correlaction time of the gramicidin channel in a lipid bilayer, *Biophys. J.* **65,** 1162–1167 (1993).
8. C. Wang, Q. Teng, and T. A. Cross, Solid-state ^{13}C NMR spectroscopy of a ^{13}C carbonyl-labeled polypeptide, *Biophys. J.* **61,** 1550–1556 (1992).
9. B. A. Cornell, F. Separovic, A. J. Baldassi, and R. Smith, Conformation and orientation of gramicidin A in oriented phospholipid bilayers measured by solid state carbon-13 NMR, *Biophys. J.* **53,** 67–76 (1988).
10. I. Solomon, Relaxation processes in a system of two spins, *Phys. Rev.* **99,** 559–565 (1955).
11. A. Kalk and H. J. C. Berendsen, Proton magnetic relaxation and spin-diffusion in proteins, *J. Magn. Reson.* **24,** 343–366 (1976).
12. D. L. Vanderhart, Natural-abundance ^{13}C–^{13}C spin exchange in rigid crystalline organic solids, *J. Magn. Reson.* **72,** 13–47 (1987).
13. S. K. Straus, T. Bremi, and R. R. Ernst, Experiments and strategies for the assignment of fully ^{13}C/^{15}N-labelled polypeptides by solid state NMR, *J. Biomol. NMR* **12,** 39–50 (1998).
14. R. R. Ernst, G. Bodenhausen, and A. Wokaun, "Principles of Nuclear Magnetic Resonance in One and Two Dimensions," Clarendon Press, Oxford (1987).
15. K. Schmidt-Rohr, Complete dipolar decoupling of ^{13}C and its use in two-dimensional double-quantum solid state NMR for determining polymer conformations, *J. Magn. Reson.* **131,** 209–217 (1998).
16. Q. Teng, M. Iqbal, and T. A. Cross, Determination of the ^{13}C chemical shift and ^{14}N electric field gradient tensor orientations with respect to the molecular frame in a polypeptide, *J. Am. Chem. Soc.* **114,** 5312–5321 (1992).
17. M. H. Levitt, D. P. Raleigh, F. Creuzet, and R. G. Griffin, Theory and simulations of homonuclear spin pair systems in rotating solids, *J. Chem. Phys.* **92,** 6347–6364 (1990).
18. R. R. Ketchem, B. Roux, and T. A. Cross, High-resolution polypeptide structure in a lamellar phase lipid environment from solid state NMR derived orientational constraints, *Structure* **5,** 1655–1669 (1997).
19. F. Tian, K.-C. Lee, W. Hu, and T. A. Cross, Monovalent cation transport: Lack of structural deformation upon cation binding, *Biochemistry* **35,** 11959–11966 (1996).
20. T. A. Cross, M. H. Frey, and S. J. Opella, ^{15}N spin exchange in a protein, *J. Am. Chem. Soc.* **105,** 7471–7473 (1983).
21. O. S. Andersen, Gramicidin channels, *Annu. Rev. Physiol.* **46,** 531–548 (1984).
22. D. D. Busath, The use of physical methods in determining gramicidin channel structure and function, *Annu. Rev. Physiol.* **55,** 473–501 (1993).
23. R. Ketchem, W. Hu, and T. A. Cross, High-resolution conformation of gramicidin A in a lipid bilayer by solid state NMR, *Science* **261,** 1457–1460 (1993).